BRAIN RESEARCH ▮ (▮▮▮▮) ▮▮▮–▮▮▮

Available online at www.sciencedirect.com

ScienceDirect

www.elsevier.com/locate/brainres

Research Report

fNIRS derived hemodynamic signals and electrodermal responses in a sequential risk-taking task

Lisa Holper[a,b,*], *Robert H.W. ten Brincke*[b], *Martin Wolf*[a], *Ryan O. Murphy*[b]

[a]*Biomedical Optics Research Laboratory (BORL), Division of Neonatology, University Hospital Zürich, Frauenklinikstrasse 10, 8091 Zürich, Switzerland*

[b]*Chair of Decision Theory and Behavioral Game Theory, Department of Humanities, Social and Political Sciences, ETH Zurich, Clausiusstrasse 50, 8092 Zürich, Switzerland*

ARTICLE INFO

Article history:
Accepted 5 February 2014

Keywords:
Dynamic decision-making
Risk-taking
Risk attitude
fNIRS
Electrodermal response

ABSTRACT

The study measured cortical hemodynamic signals and peripheral correlates of decision makers during a dynamic risky task, the *Just One More* task (JOM), in which the risky decision entails choosing whether to incrementally increase accumulated earnings at the risk of ruin (going bust ending up with nothing). Twenty subjects participated in multiple instantiations of this task in which the *probability of ruin* and size of the stakes varied. Physiological correlates were simultaneously quantified by functional near-infrared spectroscopy (fNIRS) over dorsolateral prefrontal cortex (DLPFC) and electrodermal activity (EDA). First, in the task decision phase (i.e., when subjects are contemplating options before making a choice) *probability of ruin* had a dissociating effect on fNIRS and EDA. fNIRS derived DLPFC hemodynamic signals reflected a subjective value signal, correlating positively with individual risk attitude. Contrary, EDA reflected the *probability of ruin* in terms of a common affective measure, irrespective of individuals' risk attitude. Second, during the task outcome phase (i.e., the time after subjects have made a choice and observed the outcomes) fNIRS and EDA revealed opposite patterns. While fNIRS derived DLPFC hemodynamic signals were larger in response to gains, EDA signals were larger in response to losses; both patterns were statistically independent of individual risk attitude. Lastly, fNIRS derived DLPFC hemodynamic signals in the decision phase correlated positively with the mean round earnings, providing a measure of the quality of the individual decision-making performance. Together with the positive correlation with individual risk attitude, our findings indicate that fNIRS signals, but not EDA, could be taken as a useful method for studying individual risk attitude and task performance in dynamic risky decision-making.

*Corresponding author at: University Hospital Zurich, Biomedical Optics Research Laboratory (BORL), Division of Neonatology, Frauenklinikstrasse 10, 8091 Zürich, Switzerland. Fax: +41 44 255 44 42.

E-mail addresses: holper@ini.phys.ethz.ch (L. Holper), robert.tenbrincke@gess.ethz.ch (R.H.W. ten Brincke), Martin.Wolf@usz.ch (M. Wolf), rmurphy@ethz.ch (R.O. Murphy).

http://dx.doi.org/10.1016/j.brainres.2014.02.013
0006-8993

1. Introduction

It is often necessary to make decisions under irreducible risk. In these contexts, decisions are driven by the subjective value of choice options and their respective probabilities. However, there are substantial individual differences in risk attitudes and these preferences affect the attractiveness of different choice options to different individuals. Understanding individual attitudes towards risk, and the corresponding physiological mechanisms, is therefore intimately linked to the aim of understanding decision behavior in risky contexts.

1.1. *Just One More task (JOM)*

In this study we applied a dynamic risk-taking problem, the *Just One More* task (JOM), recently introduced by Murphy and ten Brincke (2014). The JOM represents an optimal stopping problem played against nature. In the *decision phase* a decision-maker (DM) may draw one ball at a time from a randomized metaphorical urn. The virtual urn contains good balls and bad balls in a known distribution (the probability of a bad draw, referred to as the *probability of ruin* or of *going bust*, is either 0.1 or 0.2); draws are made with replacement so the probability of good and bad outcomes is constant throughout the round. A *good draw* adds a point value (the value of a good draw is either 1 or 3 and remains constant throughout the round) to the DM's accumulated total points, while a *bad draw* terminates the round and results in the DM losing all of the accumulated points for that particular round and thus earning nothing. The DM must choose when to stop making draws and bank the accumulated points, thus securing them as real earnings (there is a known exchange rate between points and pecuniary results, and we presume that the DM is motivated to earn money, more being better than less). A round is terminated by either a voluntary stop or a bad draw. Each decision phase is followed by an *outcome phase* during which feedback about the round (e.g., realized payoffs) is provided. The core of this problem for the DM is choosing when to stop making draws for incremental potential improvements and thus "walk away" and in doing so secure earnings. When this task is repeated over multiple rounds, the distribution of good/bad balls, and the number of points earned per good draw (or the exchange rate from banked points to real payoffs), can be adjusted to systematically explore the effects of value and risk (as defined here as the *probability of ruin*) on choice preferences. The JOM task is a useful tool for studying risk-taking behavior, especially for understanding how people make choices where there are low probability but high consequence negative events.

The JOM task is similar to other established risk-taking decision tasks such as the Devil's Task (Slovic, 1966), the Balloon Analog Risk Task (Lejuez et al., 2002), the Angling Risk Task (Pleskac, 2008), and the Columbia Card Task (Figner et al., 2009). In all of these decision tasks, a DMs' risk-taking preferences are assessed by observing voluntary stopping points in a series of risky choices. However, compared to these previous dynamic tasks, and other non-dynamic risk-taking tasks as well, such as the Iowa Gambling Task (Bechara et al., 1994), the Cambridge Gambling Task (Rogers et al., 1999), the Cups Task (Levin and Hart, 2003) or the Game of Dice Task (Brand et al., 2005), the JOM task has advantages as a research tool. First, whereas several of the above-mentioned tasks involve incrementally increasingly risky choices over time (i.e., draws without replacement resulting in changes in probabilities within one round), the JOM has the advantage that the *probability of ruin* remains at a constant level throughout a round. Thus the task is less cognitively demanding than other procedures where both values and probabilities are changing simultaneously. Second, the JOM facilitates computing a parameterizable index for the assessment of an individual's risk attitude. This is not possible for other common decision tasks that operate under uncertainty (e.g., the Iowa Gambling Task or the Balloon Analog Task) rather than risk. The well-specified structure of the JOM task therefore allows researchers to draw more precise conclusions about a DM's behavior and preferences than other decision tasks that have ambiguous features.

1.2. *Measures of cortical hemodynamic and peripheral decision correlates*

Decision-making under risk is theorized to require two general physiological systems: cortical and peripheral decision systems (Bechara and Damasio, 2005; Critchley, 2009). Existing studies employed either neuroimaging methods as a measure of the brain's hemodynamic correlates or electrodermal activity (EDA) as a measure of the skin's affective correlates. For isolating the effects of both systems, it has been useful to distinguish between two separate phases of a person's experience: the decision processes (the activities during the time leading up to the choice behavior) and the outcome processes (the activities after the choice behavior when outcomes and payoffs are realized).

1.2.1. *Neuroimaging as measure of cortical hemodynamic decision-making correlates*

During decision processing, neuroimaging methods, such as functional magnetic resonance imaging (fMRI), have identified the role of prefrontal areas (such as the dorsolateral, lateral and ventromedial prefrontal cortex, orbitofrontal and the anterior cingulate cortex) and subcortical areas (such as the striatum and the amygdala) in encoding the two main components of a subjective value signal, i.e., its risk probability and expected value (Fukunaga et al., 2012; Li et al., 2010; Lighthall et al., 2012; Rao et al., 2008; Schonberg et al., 2012). Typically, increasing blood-oxygen-level-dependent (BOLD) signals in these areas encode risk with respect to uncertainty, variance, or volatility (Huettel et al., 2006, 2005; Knutson et al., 2005; Preuschoff et al., 2006; Tobler et al., 2007) and encode expected value with respect to magnitude, probability, and their combination (Knutson et al., 2005; Preuschoff et al., 2006; Tobler et al., 2007). In particular, the lateral prefrontal cortex has been shown to integrate these two components into one signal that covaries with individual risk attitude (Tobler et al., 2009). In the absence of risk, hemodynamic responses in these areas increase with increasing value. The presence of risky options enhances these responses in risk-seeking individuals, but reduces them in risk-averse individuals. The interplay between risk and expected value can therefore be considered to be linked to lateral

Please cite this article as: Holper, L., et al., fNIRS derived hemodynamic signals and electrodermal responses in a sequential risk-taking task. Brain Research (2014), http://dx.doi.org/10.1016/j.brainres.2014.02.013

prefrontal cortex activity, which allows an additional means of assessing individual's risk attitudes.

During outcome processing, clusters located in traditional reward-related brain areas such as the striatum and thalamus, along with activation in prefrontal areas, are especially targeted during the experience of gains and losses (Breiter et al., 2001; Cazzell et al., 2012; Delgado et al., 2000; Lawrence et al., 2009; Lin et al., 2008; Rogers et al., 2004). Comparison of BOLD responses to gains vs. losses revealed that this network typically responds with greater activity to gains than to losses. Together, these findings on the decision and outcome processing suggest that cortical hemodynamic responses provide a subjective value signal in terms of how humans experience risky decisions.

1.2.2. *Electrodermal activity as a measure of peripheral decision-making correlates*

Contrary to the hemodynamic response reflecting a subjective value signal, the physiological system underlying EDA derived skin conductance responses (SCRs) reflects a more common affective signal (Fowles, 1986) with regard to the underlying affective response. EDA is a well-established method in decision research that offers a psychophysiological process-tracing technique of affective reactivity (Boucsein, 1992; Critchley et al., 2000; Figner and Murphy, 2010). Previous studies using EDA evaluating decision processing with respect to expected value and/or outcome variance showed that SCRs can reflect both of these factors. Both increasing expected value (Glöckner et al., 2012; Yen et al., 2012) and increasing variance in outcomes (Bechara et al., 1999; Studer and Clark, 2011; Yen et al., 2012) trigger enhanced SCRs. During outcome processing, results of the psychophysiological responses to gains and losses has furthermore shown that reward-related SCRs are modulated by the valence of outcomes (Bechara et al., 1999; Crone et al., 2004; Liao et al., 2009; Starcke et al., 2009; Tchanturia et al., 2007; Wilkes et al., 2010) and the magnitude of outcomes (Crone et al., 2004; Wilkes et al., 2010). However, in contrast to hemodynamic signals, reward-related SCRs typically show larger responses to increasing magnitude of losses compared to gains. These results show that EDA can provide both useful and complementary method to neuroimaging techniques in studying risky choice.

1.3. *Aims and hypotheses of the present study*

The majority of existing studies has investigated risk-taking behavior by focusing either on the cortical hemodynamic or the peripheral decision-making correlates independently. However, simultaneous measures evaluating the interplay between the two underlying systems can provide additional layers of information about reliable and valid ways to quantify individual risk attitudes. The present study therefore expands previous studies, first, by using a well-structured risk-taking context (e.g., the JOM task) to assess individual information-use and risk-taking behavior, and second, by assessing both the cortical hemodynamic signals and the peripheral decision-making correlates during and after choice behavior. For quantification of these decision correlates we applied functional near-infrared spectroscopy (fNIRS) and EDA. Based on previous findings, we hypothesized that (1) fNIRS and EDA signal patterns would reflect the cortical hemodynamic and peripheral characteristics of the JOM task both in the decision phase (responses to the *probability of ruin* and to the *draw value*) and the outcome phase (responses to gains and losses of potential earnings) and that (2) fNIRS, but not EDA, would provide a suitable method for quantifying individual risk attitude as previously shown for fMRI. Taken together, combining this methodological approach, we hypothesized that the cortical hemodynamic and peripheral correlates could provide both distinct effects (i.e., based on fNIRS vs. EDA signals) and risk attitude-specific information (i.e., based on fNIRS signals) of the underlying risk-taking behavior.

2. Results

2.1. *Risk attitude analysis*

Risk attitudes describe the alternative preferences people have when faced with quantified uncertainty, like risk-averse, risk-seeking or risk-neutral. To express the risk attitude for an individual subject as a single value, we assumed a utility function for money of the form $u(x)=x^{\alpha}$ and estimated the best fitting parameter of risk attitude α. We did so by minimizing the mean squared error between the subject's actual voluntary stopping points in the JOM task and the stopping points predicted by the utility function given a particular value α. Because this experimental task yields censored data, we selected only those rounds for the estimation procedure when subjects stopped voluntarily. For example, consider the instance of a subject going bust after the second draw; this observation contains little useful information regarding that subject's risk preferences. Observations were therefore corrected for the probability of reaching a particular number of draws. To see why this correction is used, consider a case where a subject intends to stop after 5 draws half of all rounds and after 7 draws for the other half of rounds. More results (e.g., voluntary stops) are likely to remain after 5 draws than after 7 draws, simply because the probability of reaching 5 draws is larger than reaching 7 draws, hence the uncorrected estimated average stopping intention would be below 6 instead of the unbiased and proper estimate of 6 draws.

The resulting α served as an index for an individual subject's risk preference, derived from their choices in the JOM. Subjects with an index value greater than 1 were defined as risk-seeking and those with an index value smaller than 1 as risk-averse. Those with a JOM-index α of exactly 1 would be defined as risk-neutral and would make choices that maximized expected value. The normative solution for the JOM task (i.e., the number of draws a risk-neutral individual who maximizes expected payoff would take) corresponds to using a draws threshold of $p/(1-p)$, where p is the probability of a good draw. The normative result is independent of the value of a good draw, and generalizes across different values of α. In other words, in the JOM, subjects should attend to the *probability of ruin* and disregard information about the value of the draws when deciding when to stop making draws. This is a notable feature of the JOM task that many other decision research contexts do not share.

Please cite this article as: Holper, L., et al., fNIRS derived hemodynamic signals and electrodermal responses in a sequential risk-taking task. Brain Research (2014), http://dx.doi.org/10.1016/j.brainres.2014.02.013

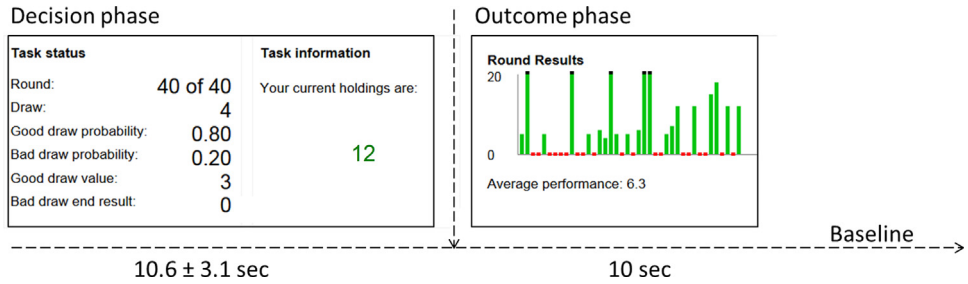

Fig. 1 – *Just One More* task (JOM): the screenshot of the JOM illustrates the end after 40 rounds. Decision phase: shown are the task status and task information describing the current progress throughout the task in terms of rounds and draws, but also provide key information regarding the task, such as the probabilities (risk) of drawing a Good Draw and a Bad Draw with the gain amount of an individual Good Draw (*Draw value* (DV)). Outcome phase: Shown are the round results (payoffs) on a 20 unit scale, with either the amount of Good Draws (GAIN=green) and Bad Draws (BUST=red).

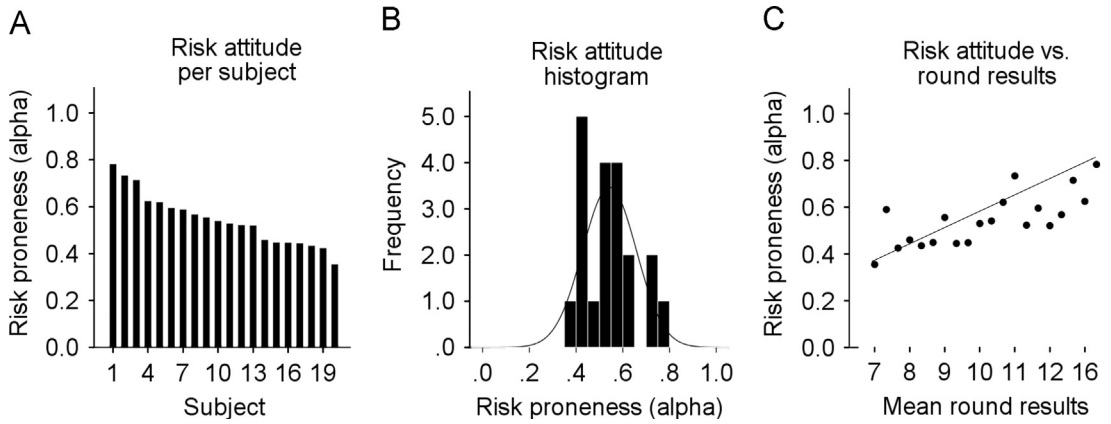

Fig. 2 – Risk attitude analysis: Illustration of individual risk attitude as represented by the JOM-index α. Based on this index (cut-off point=1) we identified only risk-averse. (A) Subjects are ordered according to the JOM-index value. (B) Histogram of the JOM-index values. (C) Mean round results for each individual JOM-index α, when considering only for voluntary stops. This plot shows a significant positive correlation ($r=0.743$, $p \leq 0.001$) indicating that the more risk-averse subjects were the smaller their mean round results were on average.

Averaged over all subjects the JOM-index α (risk attitude) was 0.543 ± 0.112 (mean $\pm$ standard deviation). Based on this index we observed only risk-averse individuals in our sample ($n=20$; 100%) (Fig. 2(A and B)). In addition, Fig. 2(C) shows the mean round results for each individual JOM-index α, when considering only voluntary stops. This plot indicates that the more risk-averse subjects were, the smaller their mean round results were on average, as indicated by the significant positive correlation ($r=0.743$, $p \leq 0.001$).

2.2. *fNIRS and EDA data*

For analysis of fNIRS and EDA, mean total hemoglobin concentration (Δ[tHb]) and SCR values were calculated per subject as dependent variables. Statistical significance was assessed using linear regression for the decision phase with the factors *probability of ruin* (PR) (LOW PR (0.1) vs. HIGH PR (0.2)) and *draw value* (DV) (LOW DV (1) vs. HIGH DV (3)) and for the outcome phase using the factor *payoff* (BUST vs. GAIN).

Fig. 3 illustrates the averaged time courses of fNIRS derived dorsolateral prefrontal cortex (DLPFC) hemodynamic signals and EDA responses of two sample subjects demonstrating both the decision and the outcome phases. In particular, the fNIRS responses show that subjects differed in signal amplitude when confronted with risky options. Using linear regression we then performed a comparison of the mean Δ[tHb] and SCRs by considering both the decision and the outcome phases (Fig. 4; Table 1).

2.2.1. *Decision phase*

With respect to the factor *probability of ruin*, fNIRS signals showed no significant differences of Δ[tHb] hemodynamic responses between low *probability of ruin* vs. high *probability of ruin* settings. In contrast, EDA data revealed significantly larger SCRs in response to high *probability of ruin* settings as compared low *probability of ruin* settings. With respect to the factor *draw value*, fNIRS data showed no significant different Δ[tHb] hemodynamic responses in low *draw value* vs. high *draw value* situations. In contrast, EDA data revealed significantly larger SCRs on average in the high *draw value* setting.

2.2.2. *Outcome phase*

Securing a positive payoff by voluntarily stopping showed a significant effect on both fNIRS signals and EDA data. fNIRS revealed significantly smaller Δ[tHb] responses to going bust as compared to gains; in contrast, the opposite pattern was

Please cite this article as: Holper, L., et al., fNIRS derived hemodynamic signals and electrodermal responses in a sequential risk-taking task. Brain Research (2014), http://dx.doi.org/10.1016/j.brainres.2014.02.013

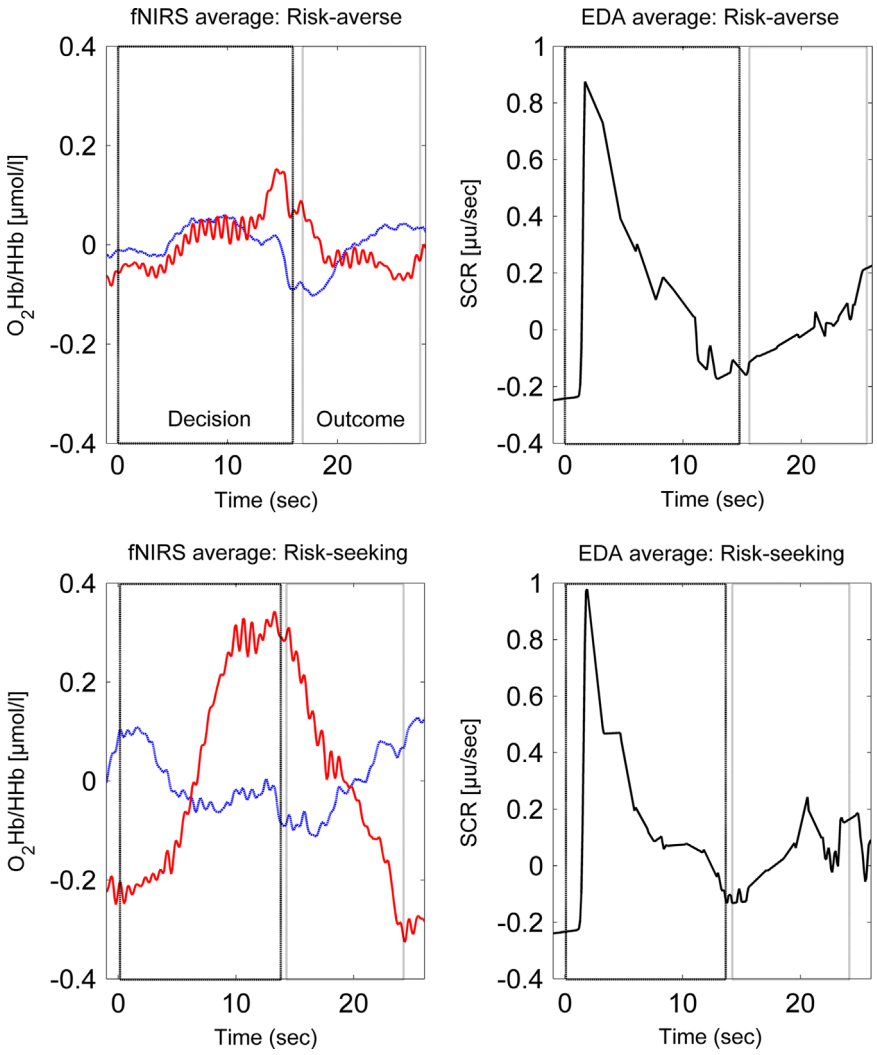

Fig. 3 – Time course: shown are the averaged time courses of fNIRS for [O_2Hb] (red) and [HHb] (blue) and of EDA for SCRs (Black) of two example subjects. Vertical lines indicate the time interval of the decision phase (long dashes) and the outcome phase (short dashes). In particular, the fNIRS responses show that subjects differed in signal amplitude when confronted with the *probability of ruin*.

found for EDA with larger SCRs for going bust as compared to realized gains.

2.3. *Correlation of risk attitude with fNIRS and EDA data*

As reported in the last section, fNIRS signals and EDA data showed differential response patterns to *probability of ruin* and *draw value*. However, results presented so far provide no indication of how these patterns would relate to individuals' risk attitudes. To assess the variation across individuals, we contrasted the distinct cortical hemodynamic and peripheral signal patterns to different levels of *probability of ruin*, *draw value* and payoff and correlated them with the JOM-index of risk attitude. In particular, we computed signal contrast estimates for fNIRS and EDA as previously described (Tobler et al., 2009), i.e., for each subject the formation of *probability of ruin*-contrasts (HIGH PR minus LOW PR), the *draw value*-contrasts (HIGH DV minus LOW DV) and payoff-contrasts (GAIN minus BUST). These contrasts were then used for computing linear correlations with the JOM-index of risk attitude.

In the decision phase, fNIRS signals showed that the *probability of ruin*-contrasts ($r=0.655$, $p=0.002$) correlated significantly positively with the JOM-index of risk attitude (Fig. 5(A)), meaning a positive correlation with greater risk-tolerant behavior. Conversely, no significant correlation was found for *draw value*-contrasts ($r=-0.073$, $p=0.759$) nor for the EDA contrasts (*probability of ruin*-contrast $r=-0.126$, $p=0.598$; *draw value*-contrast $r=-0.180$, $p=0.447$). Further, as illustrated in Fig. 5(A), we observed over all subjects significant fNIRS *probability of ruin*-contrasts in accordance with the patterns in Fig. 4 and Table 1 consisting of decreased responses to increasing *probability of ruin* (statistically significant difference between high and low *probability of ruin* options as assessed by linear regression, $R^2=0.247$, $F_2=9.989$, $p<0.001$; Beta$=$ 0.497, $t_1=4.470$, $p<0.001$). No such relation was found for EDA data. Together, these findings show that the *probability of ruin*-related fNIRS responses, but not the EDA responses,

Please cite this article as: Holper, L., et al., fNIRS derived hemodynamic signals and electrodermal responses in a sequential risk-taking task. Brain Research (2014), http://dx.doi.org/10.1016/j.brainres.2014.02.013

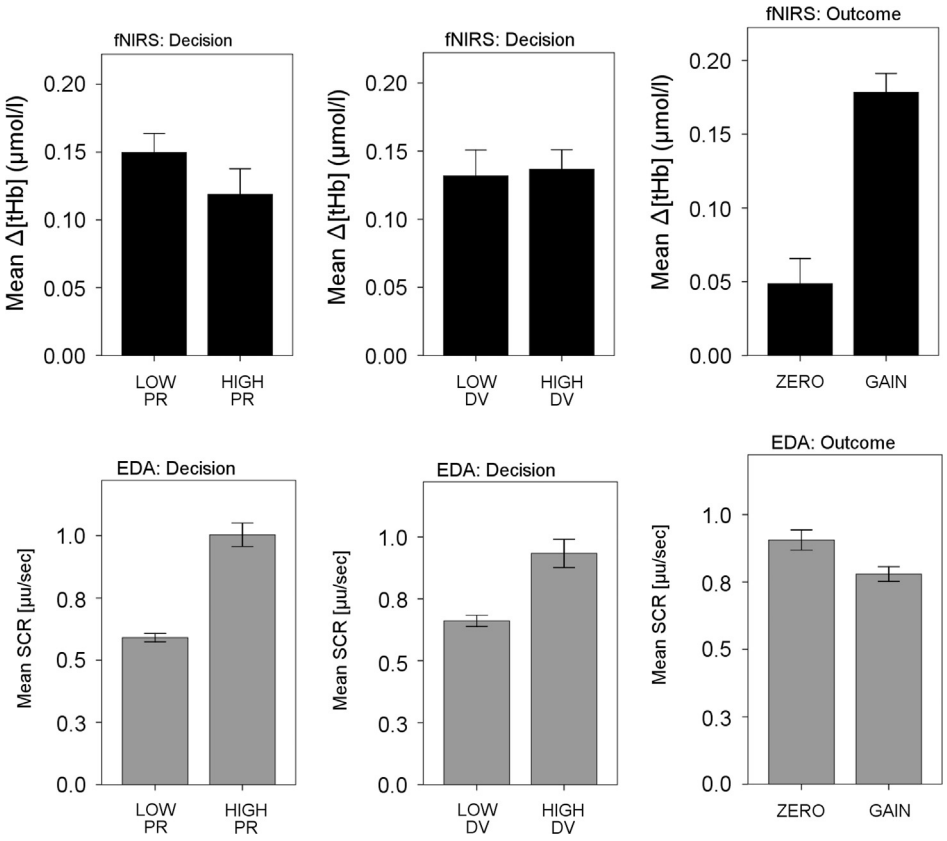

Fig. 4 – Mean responses of fNIRS and EDA signals: shown are Δ[tHb] responses (fNIRS, color black) and SCR values (EDA, color gray) in the decision phase for the factors "*Probability of ruin* (PR)" (LOW PR (0.1) vs. HIGH PR (0.2)) and "*Draw value* (DV)" (LOW DV (1) vs. HIGH DV (3)) and in the outcome phase for the factor "Payoff" (BUST vs. GAIN). Error bars indicate standard error of the mean (SEM). The corresponding analysis is listed in Table 1.

Table 1 – Mean responses of fNIRS and EDA signals: linear regression was performed with the Δ[tHb] responses and SCRs values as the dependent variables for the decision phase with the factors "*Probability of ruin* (PR)" (low PR (0.1) vs. high PR (0.2)) and "*Draw value* (DV)" (Low DV (1) vs. high DV (3)) (Top) and for the outcome phase with the factor "Payoff" (ZERO vs. GAIN) (Bottom). Listed are R^2 values, *F*-statistics with degrees of freedom (df), standardized coefficients (Beta), *t*-statistics with df and significant values ($p \leq 0.05$) are highlighted (*). Additionally partial eta squared (η_p^2) and observed post-hoc power (PHP) are shown. The corresponding plots are illustrated in Fig. 4.

		R^2	df	F	*p*-Value		
Decision phase							
Δ[tHb]		0.022	2	0.864	0.425		
SCRs		0.668	2	77.384	<0.001*		
		Beta	df	t	*p*-Value	η_p^2	PHP
Δ[tHb]	Low PR vs. high PR	−0.146	1	−1.298	0.198	0.021	0.247
	Low DV vs. high DV	0.024	1	0.211	0.834	0.001	0.055
SCRs	Low PR vs. high PR	0.682	1	10.387	<0.001*	0.726	1.000
	Low DV vs. high DV	0.450	1	6.846	<0.001*	0.536	1.000
Outcome phase							
		R^2	df	F	*p*-Value		
Δ[tHb]		0.494	1	37.084	<0.001*		
SCRs		0.164	1	7.480	0.009*		
		Beta	df	t	*p*-Value	η_p^2	PHP
Δ[tHb]	Zero vs. gain	0.703	1	6.090	<0.001*	0.494	1.000
SCRs	Zero vs. gain	−0.406	1	−2.735	0.009*	0.164	0.760

covaried with individual risk attitude in the decision phase; in particular, hemodynamic responses to high *probability of ruin* options were more reduced the more risk-averse individuals were, i.e., with higher risk aversion. Thus, the risk attitude-dependent impact was reflected in cortical hemodynamic but not the peripheral responses.

Please cite this article as: Holper, L., et al., fNIRS derived hemodynamic signals and electrodermal responses in a sequential risk-taking task. Brain Research (2014), http://dx.doi.org/10.1016/j.brainres.2014.02.013

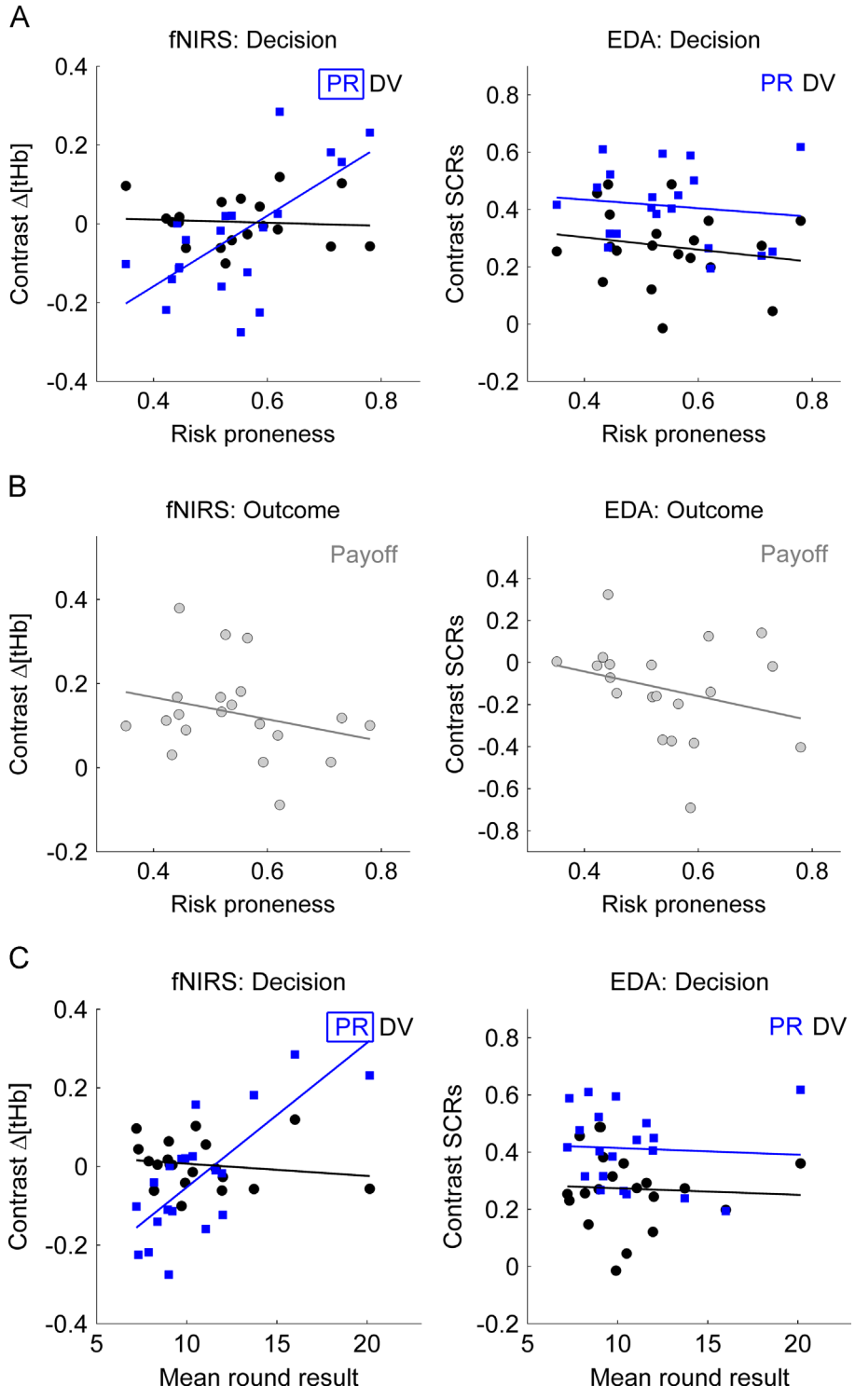

Fig. 5 – (A) Correlation with risk attitude (decision phase): plots show the correlation between the JOM-index of individual risk attitude and the signal contrasts for Δ[tHb] and SCRs (*probability of ruin* (PR)-contrasts (blue squares) and *draw value* (DV)-contrasts (black circles)). This indicated that increasing *probability of ruin* reduced fNIRS activity significantly the more risk-averse subjects were; conversely, no such effect emerged for EDA and the processing of *draw value* was also not affected by risk attitude. (B) Correlation with risk attitude (outcome phase): no significant correlation with individual risk attitude was found for payoff-contrasts (gray circles). (C) Correlation with round results (decision phase): plots show the correlation between the individual mean round results and the signal contrasts for Δ[tHb] and SCRs (PR-contrasts (blue squares) and DV-contrasts (black circles)). This indicated that increasing *probability of ruin* was associated with significantly increased fNIRS activity the higher the round results were; conversely, no such effect emerged for EDA and the processing of *draw value* was not affected by round results. In all plots significant correlations are highlighted with a square.

Please cite this article as: Holper, L., et al., fNIRS derived hemodynamic signals and electrodermal responses in a sequential risk-taking task. Brain Research (2014), http://dx.doi.org/10.1016/j.brainres.2014.02.013

In the outcome phase, no significant correlations were found for the payoff-contrasts of fNIRS ($r=-0.267$, $p=0.255$) or EDA ($r=-0.284$, $p=0.225$). Further, as illustrated in Fig. 5(B), we observed over all subjects significant fNIRS payoff-contrasts (statistical significant difference between gains and losses as assessed by linear regression, $R^2=0.602$, $F_1=45.439$, $p<0.001$; Beta=0.776, $t_1=6.741$, $p<0.001$). No such relation was found for EDA data.

2.4. Correlation of round results with fNIRS and EDA data

Lastly, in order to investigate the relationship between behavioral performance and the cortical hemodynamic and peripheral data, we calculated the mean earnings of all rounds, when considering only voluntary stops. These parameters were then applied for computing linear correlations with the signal contrast estimates for fNIRS and EDA as described above.

In addition to the positive correlation with risk attitude in the decision phase, fNIRS signals showed that the *probability of ruin*-contrasts correlated significantly positively with the mean earnings of the rounds results ($r=0.751$, $p\leq 0.001$), when considering only those rounds where subjects stopped voluntarily (Fig. 5(C)). This indicated that fNIRS signals were larger the greater the round results were. There were no significant correlations between the round results and the *draw value*-contrasts ($r=-0.160$, $p=0.500$) nor for the EDA contrasts (*probability of ruin*-contrasts $r=-0.055$, $p=0.817$; *draw value*-contrasts $r=-0.054$, $p=0.821$). Together with the positive correlation observed for risk attitude this indicated that those subjects who were more risk-neutral later obtained larger mean earnings and this was associated with greater fNIRS signals. No significant correlation was found for EDA data.

3. Discussion

We have presented behavioral, cortical hemodynamic and peripheral affective correlates of a dynamic risk-taking task, the *Just One More* task (JOM). Our experiment was motivated by the hypotheses (1) that fNIRS derived DLPFC hemodynamic signals and EDA would provide a characterization of the cortical hemodynamic and peripheral correlates in both the decision and outcome phase of the JOM and (2) that fNIRS derived DLPFC hemodynamic signals, but not EDA signals, can be used to quantify individuals' risk attitudes. Both hypotheses were accepted indicating that, based on the JOM-index as a suitable tool for assessing individual risk attitudes in a dynamic task, fNIRS provides a suitable quantification of the hemodynamic correlates of individual risk attitude.

Our results could be of relevance for future development of physiological measures of decision-making in risky contexts. fNIRS in conjunction with EDA could potentially measure the quality of the decision-making processes, in particular in cases where task performance cannot be easily judged or determined. Physiological measures could measure whether risks are taken seriously and whether subjects are sensitive to particular attributes of a given decision problem that are relevant for good decision-making. In the future, decision quality may therefore be informed by physiological results that could serve as an approximation of how well a DM is doing or what is sensible behavior in a given context. Such physiological profiles of good decision-making would be especially useful in applied settings where performance cannot be assessed directly, such as driving behavior (Jonah, 1997; Palamara et al., 2012), health behavior (Cook and Bellis, 2001; Vollrath et al., 1999), or mental illnesses (Cerimele and Katon, 2013).

3.1. Risk attitude analysis

To assess individual risk attitude we computed the JOM-index α, a metric of individual risk preferences. A small index α, i.e., not risking enough by risk-averse subjects, can result in reduced earnings, whereas a high index, i.e., more risk-taking from more risk-tolerant subjects, can lead to going bust quite often. Based on this index we observed only risk-averse individuals (Fig. 2(A)) in this particular context, but there are clear individual differences in the degree of risk-tolerance when the α index is used as a continuous variable. The distribution of subjects' preferences is consistent with previous studies that also reported the majority of people are risk-averse (Christopoulos et al., 2009; Mohr et al., 2010; Tobler et al., 2009).

3.2. fNIRS and EDA data

Regarding our first and second hypotheses, the following sections discuss the comparisons of the effects of the *probability of ruin* and *draw value* in the decision phase, followed by the effects of payoff in the outcome phase; in each case first addressing fNIRS derived Δ[tHb] responses followed by EDA derived SCR signals.

3.2.1. Relation of risk attitude with fNIRS and EDA data

3.2.1.1. *Effects of* ***probability of ruin***. Analysis of the factor *probability of ruin* showed that hemodynamic responses reflected a subjective value signal, represented by reduced responses to the *probability of ruin* the more risk-averse subjects were (Fig. 4, Table 1). This pattern correlated significantly positively with the JOM-index, indicating that *probability of ruin*-related fNIRS hemodynamic responses reflect individual's risk attitude (Fig. 5(A)). The significant positive correlation therefore relates to the missing main effect of the factor *probability of ruin*. In particular, the more risk-averse subjects were, the smaller was the fNIRS *probability of ruin*-contrast as illustrated in Fig. 5(A), and vice versa, the more subjects tended towards the risk-neutral spectrum of the JOM-index the greater was the *probability of ruin*-contrast. In this sense, we found that overall subjects elicited a typical risk-averse response pattern (small fNIRS *probability of ruin*-contrasts; statistically significant difference between high and low *probability of ruin* options). These findings are generally supported by neuroimaging (Ernst et al., 2002; Schonberg et al., 2012) reporting the involvement of lateral prefrontal cortices in risky decision-making behaviors, by brain-stimulation studies (Fecteau et al., 2007; Knoch et al., 2006) reporting that stimulation of lateral prefrontal regions alters risk attitudes and by studies in primates (Barraclough et al., 2004; Kobayashi et al., 2002; Pan et al., 2008) reporting that single lateral prefrontal neurons use reward information to

Please cite this article as: Holper, L., et al., fNIRS derived hemodynamic signals and electrodermal responses in a sequential risk-taking task. Brain Research (2014), http://dx.doi.org/10.1016/j.brainres.2014.02.013

encode reward-based stimulus. More particular, these results are in line with a previous fMRI study (Tobler et al., 2009) reporting that BOLD activity in the lateral prefrontal cortex encodes a risk attitude-dependent subjective value signal, with reduced responses to risk in risk-averse but increased responses in risk-seeking subjects.

From a psychological point of view, interpretation of the hemodynamic response patterns could be based on the typical characteristics distinguishing risk perception between risk-averse vs. risk-seeking individuals. Typically, risk-averse individuals are less comfortable with risks and therefore assign lower subjective value to taking on additional risk (more draws in the JOM) given the non-zero *probability of ruin*. Risk-averse individuals might therefore perceive escalating risk-taking as exposure to increasing possible losses, rather than exposure to the increasing potential total gain associated with additional draws (Schonberg et al., 2012). In contrast, subjects tending towards risk-seeking behavior typically see risks as challenges and thus feel excited when dealing with them; they therefore assign a relatively higher subjective value to high *probability of ruin* options. During escalating risk-taking they might therefore perceive the exposure to increasing possible gains as stimulating rather than focus on the potential lost value associated with the higher risk. Thus, the perception of potential losses vs. gains in risk-averse vs. risk-seeking subjects (which typically leads to decreased vs. increased neural activity, see Section 3.2.1.3) may therefore have been the primary trigger contributing to the observed decreased vs. increased hemodynamic responses. Together, the present data demonstrate that the behavioral analysis of individual risk attitude in relation to individual *probability of ruin*-related hemodynamic response patterns is not only viable, but can elucidate basic mechanisms of risk-taking behavior.

In contrast to the fNIRS responses, the factor *probability of ruin* elicited a different EDA pattern with SCRs magnitudes being larger in response to high- than low-risk options. This indicates that EDA reflects levels of risk, but does so irrespective of individual risk attitude (Fig. 4; Table 1), which is supported by the missing correlation with individual risk attitude (Fig. 5(A)). We therefore suggest that on the peripheral affective level all subjects of the risk attitude spectrum experience risk similarly. This is reasonable since, contrary to hemodynamic responses reflecting the subjective value, the physiological components of SCRs are expressed based on the same functional origin of the skin's eccrine activity in both subject groups, i.e., reflecting a common affective response signal (Fowles, 1986). This is in line with the well-established notion that SCRs covary with the sympathetic arousal dimension of affect, indexing its affective intensity (Figner and Murphy, 2010). However, the subjective aspects of affect, such as its valence (e.g., positive vs. negative experience) or which emotion is present (e.g., risk aversion vs. risk tolerance) are not reflected in EDA and therefore require other sources, such as the fNIRS data in the present study.

Taken together, we conclude that common affective aspects of how individuals respond to risk are reflected in EDA, while the subjective value regarding negative or positive experience towards risk are reflected in the fNIRS hemodynamic response. It should be noted that, although risk induced similar degrees of EDA in all subjects, it is still conceivable that the nature of the affect (i.e., experiencing fear vs. excitement of risk) differed between them. We therefore suggest that on the peripheral affective level subjects generally reflect (but not necessarily experience) risk similarly, whereas on the hemodynamic level risk-averse and risk-seeking subjects reflect (and experience) risk in distinct ways.

3.2.1.2. *Effects of **draw value***. Analysis of the factor *draw value* showed no effect on the hemodynamic correlates and no correlation with risk attitude (Fig. 4, Table 1). In contrast, *draw value* had a significant effect on EDA data. In particular, SCRs were found to be significantly larger in response to high vs. low *draw value*. This SCR pattern was observed with similar intensity in all subjects, indicating that *draw value* is encoded in the SCRs independent of risk attitude, an assumption that was further corroborated by the missing correlation with individual risk attitude (Fig. 5(A)).

In summary, these results indicate that different parts of the human nervous system, i.e., the central part as represented by the cortical hemodynamic responses vs. the peripheral part as represented by the electrodermal responses, respond to different aspects of the risky problem. Taken together, our data obtained in the decision phase of the JOM task confirm our first hypothesis by demonstrating that the JOM parameters can be characterized using fNIRS and EDA. Our data also confirm our second hypothesis by demonstrating that risk-related fNIRS derived hemodynamic responses, but not EDA derived responses, can be used to quantify individual risk attitude.

3.2.1.3. *Effects of payoffs*. Our data obtained in the outcome phase showed that subjects elicited larger fNIRS hemodynamic responses to gains as compared to going bust. The opposite pattern was observed in EDA data with significant larger SCRs in response to going bust as compared to gains (Fig. 4; Table 1). These results are in line with previous literature from various risk-taking tasks reporting that both BOLD activity in prefrontal areas (Bechara et al., 1999; Breiter et al., 2001; Delgado et al., 2000; Lawrence et al., 2009; Lin et al., 2008; Rogers et al., 2004) and EDA responses (Bechara et al., 1999; Crone et al., 2004; Liao et al., 2009; Starcke et al., 2009; Tchanturia et al., 2007; Wilkes et al., 2010) are especially targeted during the experience of gains and losses, however, with different response patterns consisting of larger hemodynamic signals for gains but larger SCRs for losses.

From a behavioral point of view, it has been suggested (Tom et al., 2007) that this obviously greater sensitivity of the brain to losses (decreased hemodynamic signals in our case in response to going bust) compared with gains may be directly tied to the behavioral concept of loss aversion (Kahneman and Tversky, 1979), which refers to people's tendency to strongly prefer avoiding losses to acquiring gains of equal objective value. Based on this aspect, Tom et al. (2007) showed that BOLD responses reflecting individual risk aversion could be attributed to enhanced sensitivity to losses. It should be noted that, in contrast to the study by Tom et al., the JOM task does not include real losses, only losses of potential earnings. However, if we assume that subjects "become accustomed" (i.e., establish a reference point) to the amount of holdings they have after for example three to

Please cite this article as: Holper, L., et al., fNIRS derived hemodynamic signals and electrodermal responses in a sequential risk-taking task. Brain Research (2014), http://dx.doi.org/10.1016/j.brainres.2014.02.013

five draws, we could then consider a bad draw as a loss of value (in terms of an updated reference point (Davies, 2006)). Moreover, in the context of loss aversion Tom et al. showed that the above mentioned neural sensitivity to losses is diminished in risk-neutral or risk-seeking individuals who are less loss-averse. Although it is difficult to draw conclusions based on our small sample size, the correlation analysis may reflect this lower neural sensitivity (Fig. 5(B)). If this pattern would indeed represent a risk attitude-dependence of neural sensitivity to losses, then we would have also expected to see a positive correlation with the JOM -index of risk attitude. However, no significant correlation was found; to clarify this aspect further studies are required including individuals who are more risk-tolerant.

Taken together, our data obtained in the outcome phase show that the JOM sufficiently triggers the underlying reward-related physiological cortical hemodynamic and peripheral systems in order to be detectable using fNIRS and EDA.

3.2.2. *Relation of round results with fNIRS and EDA data*

In addition to the positive correlation with risk attitude, we evaluated whether fNIRS derived DLPFC hemodynamic signals and EDA activity in the decision phase could provide a prediction of the round results in the outcome phase on an individual subject level. Our data showed that, while EDA data did not reveal a significant correlation with the round results, the fNIRS *probability of ruin*-contrasts correlated significantly positively with the mean of the rounds results for voluntary stops (Fig. 5(C)). This indicated that fNIRS signals during the decision phase were larger the greater the round results were in the outcome phase. Together with the positive correlation of fNIRS with risk attitude (i.e., risk-seeking) (Fig. 5(A)), this finding indicated that subjects who were closer to being risk-neutral obtained larger round results and this is associated with larger fNIRS activity (as shown by the *probability of ruin*-contrast).

An interpretation of these behavioral and physiological findings might be as follows. Our data may indicate that better JOM performance as measured by the round results is associated with higher fNIRS activity. Consequently the results indicate that subjects who were closer to risk-neutral performed slightly better than those who were on the very low end of the risk attitude spectrum, i.e., very risk-averse subjects. In other words, as to be expected, subjects in the middle of the continuum of the risk attitude spectrum (i.e., risk-neutral) perform better than those at the extreme ends of the continuum (i.e., risk-averse or risk-seeking). This interpretation is consistent with our risk attitude analysis (Section 2.1) suggesting that risk-neutral subjects (defined with an JOM-index of 1) maximize the expected value, while more risk-averse or more risk-seeking subjects would either leave "money on the table" or take on higher risks of going bust, respectively. In this interpretation we therefore indeed expected fNIRS activity to correlate with task performance. Individual risk preferences are an important factor in decision making performance with risk-neutrality providing generally better objective performance and realized outcomes; this performance may come at an effective cost, however, in that subjective utility is not concordantly optimized with objective expectations.

Taken together, these results may indicate that fNIRS could not only provide a measure of risk attitude based on the JOM, but may also serve as a predicative measure of individual JOM task performance. fNIRS activity during the decision phase could thus be taken as a predictive indicator whether individual risk behavior would result in lower or larger round results in the outcome phase. This conclusion should certainly be taken with care as our data can only provide evidence for the more risk-averse spectrum of the risk attitude continuum and may not generalize to risk-seeking subjects. Further studies with broader samples will be needed to close this gap.

3.3. *Conclusion*

Our findings show the potential of the *Just One More* task (JOM) as a viable diagnostic measure in the assessment of risk-taking behavior. In comparison with other risk-taking tasks, the JOM task provides the advantages of an internal assessment of individual risk attitude by means of the JOM-index. Further, our findings show that fNIRS and EDA are able to reflect the cortical hemodynamic and peripheral correlates of the JOM, indicating a dissociating effect of risk on the two underlying physiological systems. Most importantly, our data demonstrate that fNIRS hemodynamic signals, but not EDA signals, can be applied as a measure of individual risk attitude and individual task performance. Together, the JOM task in combination with the neuroscientific methods used in this study could therefore represent a suitable monitoring tool of individual risk-taking behavior.

4. Experimental procedures

4.1. *Subjects*

Twenty healthy subjects participated voluntarily in the study. All subjects (11 females, mean age (±STD) 28.9±3.9) were right-handed (mean laterality quotient (LQ±STD)=84.1±11.6) according to the Edinburgh Handedness Inventory (Oldfield, 1971). Exclusion criteria were any history of visual, neurological or psychiatric disorder or any current medication; all subjects had normal or corrected-to-normal vision. All subjects gave written informed consent. All experiments were approved by the Institutional Ethics Boards and were in accordance with the latest version of the Declaration of Helsinki.

4.2. *Just One More task (JOM)*

The JOM consists of a simple dynamic stochastic decision environment (Murphy and ten Brincke, 2014) as illustrated in Fig. 1. This is a computer controlled decision-making task that uses a virtual urn from which DMs can make draws with well-defined probabilities and outcome values. The task is structured such that most of the draws result in small gains, but there exists a constant low probability of a high impact negative event.

Prior to the experiment, subjects were given instructions about the task and the payout procedure and were presented with a few practice rounds to become familiar with the

Please cite this article as: Holper, L., et al., fNIRS derived hemodynamic signals and electrodermal responses in a sequential risk-taking task. Brain Research (2014), http://dx.doi.org/10.1016/j.brainres.2014.02.013

computer interface. Prior to the task, a baseline recording (120 s) was conducted in which subjects were asked to fixate their eyes on a fixation cross on a black screen and to remain motionless.

4.2.1. *Decision phase*

The subject may draw one ball at a time from an urn with a known distribution of good and bad outcomes. On the screen the probability of a good draw and that of a bad draw is displayed (Fig. 1). A good draw increases current holdings by a fixed amount (the *draw value*), while a bad draw results in the round ending and all of the accumulated earnings disappearing (i.e., "going bust"). There is no limit to the number of draws that a subject can make. The subject may at any time decide to choose the safe option and stop making draws, which means that the current holdings are banked (turned into real earnings) and the round ends.

One instance of this whole task is called a round, and each draw or stop decision is termed a stage. A round ends either by the subject voluntarily stopping (and banking their points into real earnings) or by going bust (and thus earning nothing). For each round in this study, the value of a good draw is either 1 or 3 and the *probability of ruin* is either 0.1 or 0.2. The particular values are determined randomly prior to each round, but remain the same throughout the stages of that round. Subjects had to register their choices on the keyboard with their right hand (9=stop; 0=draw). After each choice, the current round number, stage number, draws made and current holdings are displayed (Fig. 1). Subjects were able to make decisions without any time pressure and at their own pace (the average duration of a round (which contains multiple draws or stages) was 10.6±3.1 s, mean±standard deviation). Each subject completed 40 rounds. Rounds were independent and earnings did not carry over between rounds. Subjects knew all of these features of the decision context and there was no deception used in this research.

4.2.2. *Outcome phase*

Each decision phase was followed by an outcome phase during which feedback about the round (e.g., realized payoffs) were provided in the form of a graph (Fig. 1), showing a voluntary stop in green and a bust in red, as well as in the form of a table containing numerical results. The time interval of the outcome phase was set to a minimum of 10 s to allow for proper isolation of the cortical hemodynamic and peripheral correlates.

4.2.3. *Payment*

To ensure incentive compatibility, one round was randomly chosen at the end of the experiment for determining a subject's experimental earnings. For this selected round, subjects received their corresponding outcome and were paid in cash.

4.3. *fNIRS instrumentation and data pre-processing*

To quantify the hemodynamic decision correlates we applied a miniaturized, wireless and portable fNIRS device (Muehlemann et al., 2008). The sensor components are mounted onto a four-layer rigid-flexible printed circuit board (PCB) which, in combination with a highly flexible casing made of medical grade silicone, enables the sensor to be aligned to curved body surfaces such as the head. The size of the device is $92 \times 40 \times 22$ mm^3 and it weighs 40 g. The optical system comprises four light sources at two different wavelengths (760 nm and 870 nm) and four light detectors (PIN silicon photodiodes), resulting in four channels considered for analysis. The power is provided by a rechargeable battery, which allows continuous data acquisition for 180 min at full light emission power. The light intensity is sampled at 100 Hz and the resulting data are transmitted wirelessly to a host computer by Bluetooth within an operating range of about 5 m.

During fNIRS recording, one sensor was placed over subjects' right hemisphere, covering F4-F8 according to the International 10–20 System of Electrode Placement (Jaspers, 1958). The compact sensor measuring an area of 37.5 mm in length and 25 mm in width covered the right DLPFC. Hair under the sensor was carefully brushed away to ensure good skin contact; the sensor were fixed on subjects' heads using self-adhesive bandages which allow for a homogeneous contact pressure over the whole sensor surface (Derma Plast CoFix 40 mm).

For pre-processing of the fNIRS raw light intensity values, a program was written in MATLAB® (Version 2008a, Mathworks, Natick, Massachusetts, USA). The ambient light intensities were subtracted before taking the logarithm and low-pass filtering (7th order Chebyshev with 20 dB attenuation at 5 Hz) and the signals were then decimated to a sampling rate of 10 Hz. By applying the modified Beer–Lambert law, the concentrations of oxy-hemoglobin ($[O_2Hb]$) and deoxy-hemoglobin ([HHb]) over time were computed from the measured attenuation changes of NIR light after its transmission through tissue. These represent the dominant light absorbers for living tissue in the NIR spectral band (Delpy et al., 1988). Differential path length factors (DPF) of 6.75 for the 760 nm and 6.50 for the 870 nm light sources were applied (Zhao et al., 2002). The resulting $[O_2Hb]$ and [HHb] signals were then filtered by NIRS-SPM, a toolbox for the neuroimaging suite SPM5 (Jang et al., 2009; Tak et al., 2011, 2010; Ye et al., 2009). We applied the discrete cosine transform based detrending algorithm to remove systemic confounds and the precoloring method to remove temporal correlations using a low-pass filter (Worsley and Friston, 1995).

For statistical analysis with MATLAB® (version 2008b, The Mathworks, Natick, MA, USA) and SPSS® (Version 17.0, SPSS Inc., Chicago, USA), dependent variables were derived per subject from the $[O_2Hb]$ and [HHb] datasets averaged over all four channels. To calculate statistical significance of the task-related signal amplitudes, the mean of the baseline ($[O_2Hb]_{BASELINE}$, $[HHb]_{BASELINE}$) was subtracted from the mean of the decision phase ($[O_2Hb]_{DECISION}$, $[HHb]_{DECISION}$) and the mean of the outcome phase ($[O_2Hb]_{OUTCOME}$, $[HHb]_{OUTCOME}$), referred to as $\Delta[O_2Hb]$ and $\Delta[HHb]$. Then, $\Delta[tHb]$ was derived as the sum of the averaged $\Delta[O_2Hb]$ and $\Delta[HHb]$. $\Delta[tHb]$ was chosen as primary parameter of interest because it represents changes in blood volume, which are correlated with changes in blood flow (Grubb et al., 1974). Further, $\Delta[tHb]$ is thought to be far less sensitive to vein contamination and therefore to provide higher spatial specificity for mapping cerebral activity compared to $\Delta[O_2Hb]$ or $\Delta[HHb]$ separately (Gagnon et al., 2012).

Please cite this article as: Holper, L., et al., fNIRS derived hemodynamic signals and electrodermal responses in a sequential risk-taking task. Brain Research (2014), http://dx.doi.org/10.1016/j.brainres.2014.02.013

4.4. *EDA instrumentation and decomposition procedure*

To quantify the peripheral decision correlates an EDA system was used (Mind-Reflection, VERIM® AudioStrobe® Molinis, 16 bit resolution, range from 10 kΩ to 4.5 MΩ) that allowed for the acquisition of completely raw, unfiltered EDA data sampled at 100 Hz. Two grounded flat electrodes were attached to the distal phalange of the index and middle fingers of the left, non-dominant hand prior to recording, in order to allow EDA levels to stabilize (Fowles et al., 1981). A custom-made MATLAB® interface was used to display and event-mark the psychophysiological data.

EDA data are usually characterized by a sequence of overlapping phasic skin conductance responses (SCRs) overlying a tonic component. For full decomposition of these skin conductance (SC) data we applied the analysis software Ledalab (V3.x) (Benedek and Kaernbach, 2010) and applied continuous decomposition analysis (CDA), i.e., an extraction of the continuous phasic and tonic activity. The CDA procedure involves four steps: estimation of the tonic component, nonnegative deconvolution of phasic SC data, segmentation of driver and remainder, and reconstruction of SC data.

For statistical analysis, we focused on the phasic SCRs (average phasic driver (CDA.SCR [μu/s])). This score is thought to represent phasic activity within the response-window most accurately. SCRs were baseline corrected and a minimum amplitude criterion of 0.05 μS was used (Levinson and Edelberg, 1985).

Disclosure statement

The authors have no conflict of interest.

Acknowledgment

The authors thank all participants for assistance in carrying out this research and the Swiss Foundation for Grants in Biology and Medicine (SFGBM) and the Swiss National Science Foundation (SNSF) for financial support.

REFERENCES

Barraclough, D.J., Conroy, M.L., Lee, D., 2004. Prefrontal cortex and decision making in a mixed-strategy game. Nat. Neurosci. 7, 404–410.

Bechara, A., Damasio, A., 2005. The somatic marker hypothesis: a neural theory of economic decision. Games Econ. Behav. 52, 336–372.

Bechara, A., Damasio, A., Damasio, H., Anderson, S., 1994. Insensitivity to future consequences following damage to human prefrontal cortex. Cognition 50, 7–15.

Bechara, A., Damasio, H., Damasio, A.R., Lee, G.P., 1999. Different contributions of the human amygdala and ventromedial prefrontal cortex to decision-making. J. Neurosci. 19, 5473–5481.

Benedek, M., Kaernbach, C., 2010. Decomposition of skin conductance data by means of nonnegative deconvolution. Psychophysiology 47, 647–658.

Boucsein, W., 1992. Electrodermal Activity. Plenum Press, New York, NY.

Brand, M., Fujiwara, E., Borsutzky, S., Kalbe, E., Kessler, J., Markovitsch, H., 2005. Decision-making deficits of Korsakoff patients in a new gambling task with explicit rules: associations with executive functions. Neuropsychology 19, 267–277.

Breiter, H., Aharon, I., Kahneman, D., Dale, A., Shizgai, P., 2001. Functional imaging of neural responses to expectancy and experience of monetary gains and losses. Neuron 30, 619–639.

Cazzell, M., Li, L., Lin, Z., Patel, S., Liu, H., 2012. Comparison of neural correlates of risk decision making between genders: an exploratory fNIRS study of the Balloon Analogue Risk Task (BART). NeuroImage 62, 1896–1911.

Cerimele, J.M., Katon, W.J., 2013. Associations between health risk behaviors and symptoms of schizophrenia and bipolar disorder: a systematic review. Gen. Hosp. Psychiatry 35, 16–22.

Christopoulos, G.I., Tobler, P.N., Bossaerts, P., Dolan, R.J., Schultz, W., 2009. Neural correlates of value, risk, and risk aversion contributing to decision making under risk. J. Neurosci. 29, 12574–12583.

Cook, P., Bellis, M., 2001. Knowing the risk: relationships between risk behaviour and health knowledge. Public Health 115, 54–61.

Critchley, H., 2009. Psychophysiology of neural, cognitive and affective integration: fMRI and autonomic indicants. Int. J. Psychophysiol. 73, 88–94.

Critchley, H.D., Elliott, R., Mathias, C.J., Dolan, R.J., 2000. Neural activity relating to generation and representation of galvanic skin conductance responses: a functional magnetic resonance imaging study. J. Neurosci. 20, 3033–3040.

Crone, E.A., Somsen, R., Van Beek, B., Van Der Molen, M., 2004. Heart rate and skin conductance analysis of antecedents and consequences of decision-making. Psychophysiology 41, 531–540.

Davies, G., 2006. Dynamic Reference Points: Investors as Consumers of Information (Working Paper). University College London.

Delgado, M., Nystrom, L., Fissell, C., Noll, D., Fiez, J., 2000. Tracking the hemodynamic responses to reward and punishment in the striatum. J. Neurophysiol. 84, 3072–3077.

Delpy, D., Cope, M., Zee, P., Arridge, S., Wray, S., Wyatt, J., 1988. Estimation of optical pathlength through tissue from direct time of flight measurement. Phys. Med. Biol. 33, 1433–1442.

Ernst, M., Bolla, K., Mouratidis, M., Contoreggi, C., Matochik, J., Kurian, V., Cadet, J., Kimes, A., London, E., 2002. Decision-making in a risk-taking task: a PET study. Neuropsychopharmacology 26, 682–691.

Fecteau, S., Pascual-Leone, A., Zald, D.H., Liguori, P., Théoret, H., Boggio, P.S., Fregni, F., 2007. Activation of prefrontal cortex by transcranial direct current stimulation reduces appetite for risk during ambiguous decision making. J. Neurosci. 27, 6212–6218.

Figner, B., Mackinlay, R., Wilkening, F., Weber, E., 2009. Affective and deliberative processes in risky choice: age differences in risk taking in the Columbia Card Task. J. Exp. Psychol.: Learn. Mem. Cognit. 35, 709–730.

Figner, B., Murphy, R., 2010. Using skin conductance in judgment and decision making research. In: Schulte-Mecklenbeck, M., Kuehberger, A., Ranyard, R. (Eds.). A Handbook of Process Tracing Methods for Decision Research.

Fowles, D., 1986. The eccrine system and electrodermal activity, Psychophysiology. Guilford Press, New York51–96.

Fowles, D.C., Christie, M.J., Edelberg, R., Grings, W.W., Lykken, D.T., Venables, P.H., 1981. Publication recommendations for electrodermal measurements. Psychophysiology 18, 232–239.

Fukunaga, R., Brown, J., Bogg, T., 2012. Decision making in the Balloon Analogue Risk Task (BART): Anterior cingulate cortex

signals loss aversion but not the infrequency of risky choices. Cognit. Affect. Behav. Neurosci. 12, 479–490.

Gagnon, L., Yücel, M.A., Dehaes, M., Cooper, R.J., Perdue, K.L., Selb, J., Huppert, T.J., Hoge, R.D., Boas, D.A., 2012. Quantification of the cortical contribution to the NIRS signal over the motor cortex using concurrent NIRS-fMRI measurements. NeuroImage 59, 3933–3940.

Glöckner, A., Fiedler, S., Hochman, G., Ayal, S., Hilbig, B., 2012. Processing differences between descriptions and experience: a comparative analysis using eye-tracking and physiological measures. Front. Psychol. 3, 173.

Grubb, R., Raichle, M., Eichling, J., Ter-Pogossian, M., 1974. The effects of changes in $PaCO_2$ cerebral blood volume, blood flow, and vascular mean transit time. Stroke 5, 630–639.

Huettel, S., Song, A., McCarthy, G., 2005. Decisions under uncertainty: probabilistic context influences activation of prefrontal and parietal cortices. J. Neurosci. 25, 3304–3311.

Huettel, S., Stowe, C., Gordon, E., Warner, B., Platt, M., 2006. Neural signatures of economic preferences for risk and ambiguity. Neuron 49, 765–775.

Jang, K., Tak, S., Jung, J., Jang, J., Jeong, Y., Ye, J., 2009. Wavelet minimum description length detrending for near-infrared spectroscopy. J. Biomed. Opt. 14, 034004.

Jaspers, H., 1958. The ten-twenty electrode system of the International Federation. Electroencephalogr. Clin. Neurophysiol. 10, 371–375.

Jonah, B.A., 1997. Sensation seeking and risky driving: a review and synthesis of the literature. Accid. Anal. Prev. 29, 651–665.

Kahneman, D., Tversky, A., 1979. Prospect theory: an analysis of decision under risk. Econometrica 47, 263–291.

Knoch, D., Gianotti, L.R.R., Pascual-Leone, A., Treyer, V., Regard, M., Hohmann, M., Brugger, P., 2006. Disruption of right prefrontal cortex by low-frequency repetitive transcranial magnetic stimulation induces risk-taking behavior. J. Neurosci. 26, 6469–6472.

Knutson, B., Taylor, J., Kaufmann, M., Peterson, R., Glover, G., 2005. Distributed neural representation of expected value. J. Neurosci. 25, 4806–4812.

Kobayashi, S., Lauwereyns, J., Koizumi, M., Sakagami, M., Hikosaka, O., 2002. Influence of reward expectation on visuospatial processing in macaque lateral prefrontal cortex. J. Neurophysiol. 87, 1488–1498.

Lawrence, N., Jollant, F., O'Daly, Q., Zaleya, F., Phillips, M., 2009. Distinct roles of prefrontal cortical subregions in the Iowa Gambling Task. Cereb. Cortex 19, 1134–1143.

Lejuez, C., Read, J., Kahler, C., Richards, J., Ramsey, S., Stuart, G., Strong, D., Brown, R., 2002. Evaluation of a behavioral measure of risk taking: The Balloon Analog Risk Task (BART). J. Exp. Psychol.: Appl. 8, 75–84.

Levin, I., Hart, S., 2003. Risk preferences in young children: Early evidence of individual differences in reaction to potential gains and losses. J. Behav. Decision Making 16, 397–413.

Levinson, D.F., Edelberg, R., 1985. Scoring criteria for response latency and habituation in electrodermal research: a critique. Psychophysiology 22, 417–426.

Li, X., Lu, Z., D'Argembeau, A., Ng, M., Bechara, A., 2010. The Iowa gambling task in fMRI images. Hum. Brain Mapp. 31, 410–423.

Liao, P., Uher, R., Lawrence, N., Treasure, J., Schmidt, U., Campbell, I., Collier, D., Tchanturia, K., 2009. An examination of decision making in bulimia nervosa. J. Clin. Exp. Neuropsychol. 31, 455–461.

Lighthall, N., Sakaki, M., Vasunilashorn, S., Nga, L., Somayajula, S., Chen, E., Samii, N., Mather, M., 2012. Gender differences in reward-related decision processing under stress. Soc. Cognit. Affect. Neurosci. 7, 476–484.

Lin, C., Chiu, Y., Cheng, C., Hsieh, J., 2008. Brain maps of Iowa gambling task. BMC Neurosci. 9, 72.

Mohr, P., Biele, G., Krugel, L., Li, S., Heekeren, H., 2010. Neural foundations of risk-return trade-off in investment decisions. NeuroImage 49, 2556–2563.

Muehlemann, T., Haensse, D., Wolf, M., 2008. Wireless miniaturized in-vivo near infrared imaging. Opt. Express 16, 10323–10330.

Murphy, R., ten Brincke, R., 2014. Bonuses bite back: How competitive incentives make everyone worse off. Working paper, Chair of Decision Theory and Behavioral Game Theory, ETH Zürich.

Oldfield, R., 1971. The assessment and analysis of handedness: the Edinburgh inventory. Neuropsychologia 9, 97–113.

Palamara, P., Molnar, L., Eby, D., Kopinanthan, C., Langford, J., Gorman, J., Broughton, M., 2012. Review of Young Driver Risk Taking and its Association with Other Risk Taking Behaviours (No. RR 1). Curtin-Monash Accident Research Centre.

Pan, X., Sawa, K., Tsuda, I., Tsukada, M., Sakagami, M., 2008. Reward prediction based on stimulus categorization in primate lateral prefrontal cortex. Nat. Neurosci. 11, 703–712.

Pleskac, T., 2008. Decision making and learning while taking sequential risks. J. Exp. Psychol.: Learn. Mem. Cognit. 34, 167–185.

Preuschoff, K., Bossaerts, P., Quartz, S., 2006. Neural differentiation of expected reward and risk in human subcortical structures. Neuron 51, 381–390.

Rao, H., Korcykowski, M., Pluta, J., Hoang, A., Detre, J., 2008. Neural correlates of voluntary and involuntary risk taking in the human brain: an fMRI study of the Balloon Analog Risk Task (BART). NeuroImage 42, 902–910.

Rogers, R., Owen, A., Middleton, H., Williams, E., Pickard, J., Sahakian, B., Robbins, T., 1999. Choosing between small, likely rewards and large, unlikely rewards activates inferior and orbital prefrontal cortex. J. Neurosci. 19, 9029–9038.

Rogers, R., Ramnani, N., Mackay, C., Wilson, J., Jezzard, P., Carter, C., Smith, S., 2004. Distinct portions of anterior cingulate cortex and medial prefrontal cortex are activated by reward processing in separable phases of decision-making cognition. Biol. Psychiatry 55, 594–602.

Schonberg, T., Fox, C., Mumford, J., Congdon, E., Trepel, C., Poldrack, R., 2012. Decreasing ventromedial prefrontal cortex activity during sequential risk-taking: an fMRI investigation of the balloon analog risk task. Front. Neurosci., 6.

Slovic, P., 1966. Risk-taking in children: age and sex differences. Child Dev. 37, 169–176.

Starcke, K., Tuschen-Caffier, B., Markowitsch, H., Brand, M., 2009. Skin conductance responses during decisions in ambiguous and risky situations in obsessive-compulsive disorder. Cognit. Neuropsychiatry 14, 199–216.

Studer, B., Clark, L., 2011. Place your bets: psychophysiological correlates of decision-making under risk. Cognit. Affect. Behav. Neurosci. 11, 144–158.

Tak, S., Jang, J., Lee, K., Ye, J., 2010. Quantification of CMRO(2) without hypercapnia using simultaneous near-infrared spectroscopy and fMRI measurements. Phys. Med. Biol. 55, 3249–3269.

Tak, S., Yoon, S., Jang, J., Yoo, K., Jeong, Y., Ye, J., 2011. Quantitative analysis of hemodynamic and metabolic changes in subcortical vascular dementia using simultaneous near-infrared spectroscopy and fMRI measurements. NeuroImage 55, 176–184.

Tchanturia, K., Liao, P., Uher, R., Lawrence, N., Treasure, J., Campbell, I., 2007. An investigation of decision making in anorexia nervosa using the Iowa Gambling Task and skin conductance measurements. J. Int. Neuropsychol. Soc. 13, 635–641.

Tobler, P.N., Christopoulos, G.I., O'Doherty, J.P., Dolan, R.J., Schultz, W., 2009. Risk-dependent reward value signal in human prefrontal cortex. Proc. Natl. Acad. Sci. 106, 7185–7190.

Please cite this article as: Holper, L., et al., fNIRS derived hemodynamic signals and electrodermal responses in a sequential risk-taking task. Brain Research (2014), http://dx.doi.org/10.1016/j.brainres.2014.02.013

Tobler, P.N., O'Doherty, J.P., Dolan, R.J., Schultz, W., 2007. Reward value coding distinct from risk attitude-related uncertainty coding in human reward systems. J. Neurophysiol. 97, 1621–1632.

Tom, S.M., Fox, C.R., Trepel, C., Poldrack, R.A., 2007. The neural basis of loss aversion in decision-making under risk. Science 315, 515–518.

Vollrath, M., Knoch, D., Cassano, L., 1999. Personality, risky health behaviour, and perceived susceptibility to health risks. Eur. J. Pers. 13, 39–50.

Wilkes, B., Gonsalvez, C., Blaszcynski, A., 2010. Capturing SCL and HR changes to win and loss events during gambling on electronic machines. Int. J. Psychophysiol. 78, 265–272.

Worsley, K.J., Friston, K., 1995. Analysis of fMRI time-series revisited—again. NeuroImage 2, 173–181.

Ye, J.C., Tak, S., Jang, K.E., Jung, J., Jang, J., 2009. NIRS-SPM: statistical parametric mapping for near-infrared spectroscopy. NeuroImage 44, 428–447.

Yen, N., Chou, I., Chung, H., Chen, K., 2012. The interaction between expected values and risk levels in a modified Iowa gambling task. Biol. Psychol. 91, 232–237.

Zhao, H., Tanikawa, Y., Gao, F., Onodera, Y., Sassaroli, A., Tanaka, K., Yamada, Y., 2002. Maps of optical differential pathlength factor of human adult forehead, somatosensory motor and occipital regions at multi-wavelengths in NIR. Phys. Med. Biol. 47, 2075–2093.

Please cite this article as: Holper, L., et al., fNIRS derived hemodynamic signals and electrodermal responses in a sequential risk-taking task. Brain Research (2014), http://dx.doi.org/10.1016/j.brainres.2014.02.013